Imaging, Diagnosis, Prognosis

Clinical Cancer Research

Specific PET Imaging of x_C^- Transporter Activity Using a ^{18}F-Labeled Glutamate Derivative Reveals a Dominant Pathway in Tumor Metabolism

Norman Koglin, Andre Mueller, Mathias Berndt, Heribert Schmitt-Willich, Luisella Toschi, Andrew W. Stephens, Volker Gekeler, Matthias Friebe, and Ludger M. Dinkelborg

Abstract

Purpose: ^{18}F-labeled small molecules targeting adaptations of tumor metabolism possess the potential for early tumor detection with high sensitivity and specificity by positron emission tomography (PET) imaging. Compounds tracing deranged pathways other than glycolysis may have advantages in situations where 2-[^{18}F]fluoro-2-deoxy-D-glucose (FDG) has limitations. The aim of this study was the generation of a metabolically stable ^{18}F-labeled glutamate analogue for PET imaging of tumors.

Experimental Design: Derivatives of L-glutamate were investigated in cell competition assays to characterize the responsible transporter. An automated radiosynthesis was established for the most promising candidate. The resulting ^{18}F-labeled PET tracer was characterized in a panel of *in vitro* and *in vivo* tumor models. Tumor specificity was investigated in the turpentine oil-induced inflammation model in rats.

Results: A fluoropropyl substituted glutamate derivative showed strong inhibition in cell uptake assays. The radiosynthesis was established for (4*S*)-4-(3-[^{18}F]fluoropropyl)-L-glutamate (BAY 94-9392). Tracer uptake studies and analysis of knockdown cells showed specific transport of BAY 94-9392 via the cystine/glutamate exchanger designated as system x_C^-. No metabolites were observed in mouse blood and tumor cells. PET imaging with excellent tumor visualization and high tumor to background ratios was achieved in preclinical tumor models. In addition, BAY 94-9392 did not accumulate in inflammatory lesions in contrast to FDG.

Conclusions: BAY 94-9392 is a new tumor-specific PET tracer which could be useful to examine system x_C^- activity *in vivo* as a possible hallmark of tumor oxidative stress. Both preclinical and clinical studies are in progress for further characterization. *Clin Cancer Res; 17(18); 6000–11. ©2011 AACR.*

Introduction

Tumors depend on specific adaptations in their intermediary metabolism and efficient detoxification processes to assure survival and proliferation in a challenging microenvironment and during treatment with toxic chemotherapeutic agents. Otto Warburg recognized enhanced breakdown of glucose in tumors compared with normal tissues almost 100 years ago (1). The increased glycolytic activity observed in many tumors is only one adaptation mechanism, other ones have been subsequently elucidated (2, 3). For example, aerobic glycolysis in tumors is associated with the lipogenesis and glutaminolytic pathway to provide key intermediates for anabolic reactions. Multiple mechanisms converge to support rapid energy generation, to increase biosynthesis of macromolecules, maintain appropriate cellular redox status, and detoxification potential (4). Figure 1 provides a simplified scheme on major metabolic pathways in tumors and their interrelationship. Glucose and glutamine are the major carbon and energy sources used for growth and proliferation of tumor cells. The contribution of each pathway and the flux rate of breakdown may differ among tumors. High intracellular levels of L-glutamate result from an inwardly directed concentration gradient of L-glutamine and its subsequent deamidation by glutaminase. L-glutamate is further metabolized via 3 main pathways: (i) during glutaminolysis, (ii) for glutathione (GSH) biosynthesis, and (iii) as exchange substrate for system x_C^-. As part of the cellular detoxification system, system x_C^- and GSH play an important role for protection against reactive oxygen species (ROS) and tumor survival during therapy.

Authors' Affiliation: Global Drug Discovery, Bayer HealthCare, Berlin, Germany

Note: Supplementary data for this article are available at Clinical Cancer Research Online (http://clincancerres.aacrjournals.org/).

Corresponding Author: Ludger M. Dinkelborg, Muellerstr. 178, 13353 Berlin, Germany. Phone: 49-30-468-17404; Fax: 49-30-468-16609; E-mail: ludger.dinkelborg@bayer.com

doi: 10.1158/1078-0432.CCR-11-0687

Translational Relevance

The specific localization and better characterization of tumors in patients remain important unmet medical needs, which can be hypothetically addressed by assessment of system x_C^- activity. Here we show that a novel ^{18}F-radiolabeled L-glutamate analogue, BAY 94-9392, is specifically transported via system x_C^- and can be used for visualization of tumors by positron emission tomography (PET) imaging. It shows high and specific accumulation in preclinical tumor models. The prevalence and degree of uptake in many different tumor cell lines and tumor xenografts point to the importance of this transport. BAY 94-9392 has the potential to be used clinically for tumor diagnosis because of the high tumor to background ratio and low uptake in healthy tissues. In addition, its uptake provides insight into the metabolic requirements of tumors and may provide opportunities to assess detoxification potential and survival pathways to better guide new and existing therapeutic interventions. PET imaging studies using BAY 94-9392 could contribute to elucidate the role of system x_C^- in oxidative stress and chemoresistance.

The increased uptake of glucose and its enhanced metabolism is commonly used for tumor imaging with positron emission tomography (PET) using the radiolabeled analogue 2-[^{18}F]fluoro-2-deoxy-D-glucose (FDG; ref. 5). This compound is avidly taken up and phosphorylated by tumors. The substitution at the C-2 position of FDG results in an intracellular trapping of the tracer, because further metabolism and efflux of phosphorylated FDG is hampered. The fate of FDG can be followed noninvasively *in vivo* by PET imaging and has been implemented as a valuable tool in the clinical routine (6). Today FDG is by far the most often applied PET tracer worldwide, although it has several pitfalls and limitations. A major limitation of this tracer is posed by the nonspecificity toward inflammation. In addition, enhanced uptake of FDG occurs in inflamed tissues around tumors treated with radiation therapy or in scar tissue following surgery, impeding early response assessment. FDG also accumulates in several tissues possessing an increased glucose metabolism such as brain, heart, and brown adipose tissue (7). Moreover, FDG does not accumulate in tumors with low glycolytic activities, such as prostate cancer, and can not be used for the specific detection of brain tumors and brain metastases because of a high background from healthy brain glucose metabolism. To overcome these limitations of FDG, common adaptations of the tumor metabolism beyond enhanced glycolysis need to be exploited to provide an improved PET imaging agent for tumors. Suitable PET tracers might be very helpful to shed more light on those adaptations as they can be directly translated and further investigated in patients for an earlier diagnosis and a better treatment of oncological diseases.

Tumors in general often have to cope with severe conditions of oxidative stress. Thiol-containing molecules like the amino acid L-cysteine and the tripeptide GSH are the major cellular components to overcome these conditions and are consumed for detoxification of ROS and other electrophiles, such as chemotherapeutics (8). GSH is one of the most abundant intracellular small molecules showing intracellular concentrations in the millimolar range and is considered as the major natural antioxidant (9). A continuous supply of GSH and its precursors are critical for cell survival and provide a selective advantage for tumor growth. L-cysteine plays a key role as ROS scavenger by itself and is the rate-limiting building block for GSH biosynthesis (10). Furthermore, it is part of the cystine/cysteine redox cycle for maintaining redox balance (Fig. 1; refs. 11, 12). In the blood, the oxidized dimer L-cystine is the dominant form and the availability of L-cysteine is limited. However, L-cystine can be efficiently provided to cells via the cystine/glutamate exchanger. This transporter, now referred to as system x_C^-, was first described by Bannai and Kitamura in 1980 as a sodium-independent, high-affinity transporter for L-cystine and L-glutamate in human fibroblasts (13). System x_C^- is a heterodimeric transporter consisting of 2 subunits, the light chain xCT (SLC7A11) conferring substrate specificity and the heavy chain 4F2hc (SLC3A2) which is part of several heterodimeric amino acids transporters (14). SLC3A2 is responsible for their proper membrane localization and activity (15).

After uptake of L-cystine into cells it is reduced to 2 molecules of L-cysteine (16). It is important to note that system x_C^- is not able to discriminate between its natural substrates L-cystine and L-glutamate for the inward directed transport (17). An increased expression of system x_C^- is found in many tumors, providing a survival advantage by increasing access to L-cysteine via the extracellularly more abundant L-cystine (18). The concentration of L-glutamate in tumor cells can be as high as 20 mmol/L (19, 20). This high glutamate concentration is derived primarily from high uptake of L-glutamine and an enhanced glutaminolytic pathway. L-glutamate serves here as a readily available intracellular exchange substrate for the system x_C^- and supports the efficient provision of the sulfur-containing precursor for GSH biosynthesis. In addition to its role as exchange substrate, L-glutamate is either directly consumed in the glutathione biosynthesis or serves as an anaplerotic substrate to refill the tricarboxylic acid (TCA) cycle intermediate alpha-ketoglutarate (αKG) after transamination (Fig. 1).

We hypothesized that the enhanced expression and activity of system x_C^- in tumors represent an attractive opportunity to be exploited for PET tracer discovery. To this end, we assessed suitable compounds targeting system x_C^- for the incorporation of a radioactive PET isotope. The PET radioisotope of choice for radiolabeling of small molecules is fluorine-18 based on its favorable nuclear characteristics and short half-life ($t_{1/2}$ = 110 minutes; ref. 21). However, some structural prerequisites need to be considered to assure direct radiolabeling with ^{18}F in a high yield for subsequent clinical application. Several structural

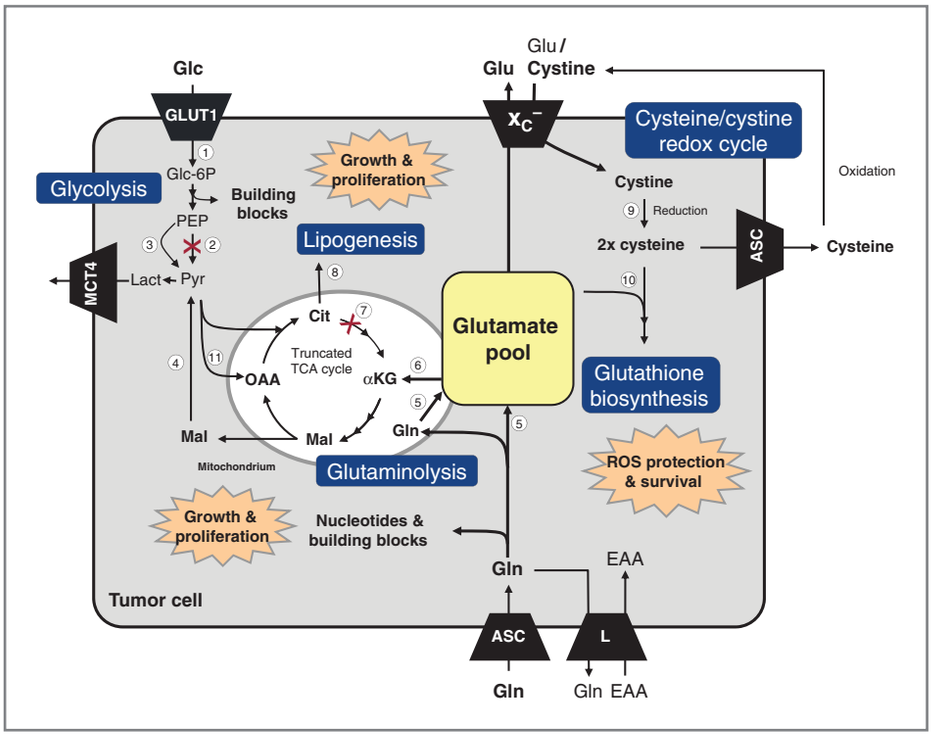

Figure 1. Tumor-specific adaptations of intermediary metabolism for assuring growth, proliferation, and survival. Tumors are characterized by adaptation of several catabolic and anabolic pathways to meet their demands for energy, growth, proliferation, and detoxification. In particular, pathways comprising glycolysis, lipogenesis, glutaminolysis, and glutathione biosynthesis are pronounced. The TCA cycle in tumors is mostly truncated leading to the efflux of mitochondrial citrate into the cytosol providing carbons for lipogenesis (43). Here, L-glutamate serves as the major anaplerotic substrate to refuel the TCA cycle. L-glutamate is obtained from glutamine degradation via glutaminase and accumulates intracellularly at high concentrations (19, 20). In addition, L-glutamate is one component of the tripeptide GSH and is consumed for its biosynthesis or is used as an exchange substrate for the uptake of L-cystine via the system x_C^- transporter. Abbreviations: 1, hexokinase; 2, pyruvate kinase–M2 isoform (PK-M2; refs. 44, 45); 3, enzyme described, but not identified yet (46); 4, malic enzyme; 5, glutaminase; 6, glutamate transaminases (GOT/GPT) and/or glutamate dehydrogenase; 7, aconitase; 8, lipogenesis pathway (ATP-citrate lyase, acetyl CoA carboxylase, and fatty acid synthase); 9, thioredoxin/thioredoxin reductases; 10, gamma-glutamyl cysteine synthetase; 11, pyruvate carboxylase (ref. 47); amino acid transport systems: system ASC, comprising for example ASCT2 (SLC1A5); system L, heterodimer consisting of LAT1 (SLC7A5) and 4F2hc (SLC3A2) subunits; system x_C^-, heterodimer consisting of xCT (SLC7A11) and 4F2hc (SLC3A2) subunits; Cit, citrate; EAA, essential amino acids; Glc, glucose; Glu, glutamate; Gln, glutamine; Lact, lactate; Mal, malate; OAA, oxaloacetic acid; PEP, phosphoenol pyruvate; Pyr, pyruvate.

analogues of L-cystine and L-glutamate are reported to be either substrates or inhibitors for system x_C^- (17). However, L-cystine itself with its disulfide bond seems suboptimal for direct and robust ^{18}F-radiolabeling. The x_C^- inhibitors p-carboxyphenylglycine and sulfasalazine are disadvantageous because of their low binding affinities (17, 22). Therefore, we focused our research on substrate compounds such as fluorinated derivatives of L-glutamate. We recently presented promising preclinical and clinical results from 4-[^{18}F]fluoro L-glutamate (BAY 85-8050) for tumor imaging (23, 27). This derivative is transported by both, the system x_C^- and the sodium-dependent glutamate transporters from the excitatory amino-acid transporter (EAAT) family. Although intriguing tumor uptake was seen, the compound was defluorinated in humans resulting in suboptimal images. For assessment of system x_C^- activity, a derivative is needed that is solely transported via this system. The aim of this study is to explore the underlying biology and transport mechanisms in more detail and to provide a metabolically stable PET tracer.

Materials and Methods

General

The tumor cell lines were obtained from ATCC or DSZM if not otherwise indicated and maintained according to protocols provided by the supplier. All chemicals were obtained from Sigma-Aldrich, Tocris Bioscience, Alexis Biochemical (now Enzo Life Sciences), Bachem AG, Toronto Research Chemicals Inc., Acros Organics (part of Thermo Fisher-Scientific). [3,4-^{3}H]L-glutamate (1.85 TBq/mmol) was purchased from Perkin Elmer and [1-^{14}C]L-cystine (3.7 GBq/mmol) was obtained from American Radiolabeled Chemicals via Biotrend.

Chemistry and radiochemistry

The nosylate precursor di-tert-butyl (4*S*)-*N*-(tert-butoxycarbonyl)-4-(3-{[(4-nitrophenyl) sulfonyl]oxy}propyl)-L-glutamate was obtained in 3 steps starting from di-tert-butyl-*N*-(tert-butoxycarbonyl)-L-glutamate (24, 25).

Radiolabeling of BAY 94-9392 was accomplished by nucleophilic substitution using $K^{18}F$ kryptofix complex and subsequent acidic deprotection followed by cartridge purification. More detailed chemistry information can be found in the supplementary information file and was published recently in a patent application (26).

In vitro tracer uptake and competition studies

For tracer uptake and competition studies, the tumor cells were seeded in 48-well plates at appropriate concentrations. The cell number used for seeding was adjusted for every tumor cell line to yield approximately 100,000 cells at the day of uptake study. Cells were usually grown for 2 to 3 days under standard conditions (37°C, 5% CO_2) until subconfluency. The cell number at the day of the uptake assay was determined by detaching cells in 3 representative wells and cell counting in a Neubauer cell chamber. Uptake data were normalized to 100,000 cells. Prior to the radioactive uptake assay, the cell culture medium was removed and the cells were washed twice with PBS buffer. Radiotracers were added to the assay buffer (PBS/0.1% w/v bovine serum albumin) by using 250 kBq/well for ^{18}F-labeled compounds, 37 kBq/well for [^{3}H]-L-glutamate, and 3.7 kBq/well for [^{14}C]L-cystine. For competition experiments, the cells were coincubated with competitors either in excess at 1 mmol/L or in a dose-dependent manner (0.0002 – 1 mmol/L). Tracer uptake was stopped by removal of the assay buffer at the time points indicated. Cells were quickly washed twice with PBS and lysed by the addition of 1 N NaOH. The cell lysate was removed from the plates. Radioactivity of ^{18}F-samples was determined in a gamma counter (Wizard 3, Perkin Elmer). ^{14}C and ^{3}H containing samples were measured in a beta counter (TriCarb 2900TR, Perkin Elmer) after addition of a liquid scintillation cocktail. For transstimulation assays, cells were loaded with BAY 94-9392 for 30 minutes, washed, and incubated with compounds at 1 mmol/L for 30 minutes in PBS. Cell associated and radioactivity released in the supernatant were measured in a gamma counter.

Generation of xCT knockdown cells

A549 human lung adenocarcinoma cells for xCT knockdown experiments were obtained from European Collection of Animal Cell Cultures and maintained in Dulbecco's modified Eagle's medium/Ham's F12 plus L-glutamine (PAA Laboratories) supplemented with 10% fetal calf serum (PAA Laboratories).

A549 cells were transduced with lentiviruses encoding short hairpin RNAs (shRNA) to human xCT mRNA sequence and to a "scramble" nontargeting sequence as a control. shRNA fragments were cloned in a lentivirus vector under the control of a U6 promoter (ViraPower Gateway system from Invitrogen) and carrying puromycin as antibiotic resistance marker. shRNA sequences were selected from human xCT mRNA NM_014331. The corresponding shRNA numbers refer to the position on NM_014331 sequence:

shRNA-1487: -AGTTGCTGGGCTGATTTAT-
shRNA-7701: -TCATACTCGACTAGAAACG-

As nonsilencing control shRNA the scramble sequence from QIAGEN (QIAGEN GmbH) was cloned in the same lentivirus plasmid backbone.

A549 cells were seeded on a 6-well plate (200,000 cells/well) for lentivirus transduction. Twenty-four hours later the culture medium was replaced with the lentivirus-containing medium (virus concentration 1 μg/mL) and incubated for 6 hours. Upon virus transduction, the incubation medium was removed and fresh culture medium was added to the cells. Seventy-two hours after transduction, puromycin-containing medium (1 μg/mL) was added to the cells. After completion of selection the cell samples were collected and xCT silencing was monitored by real time quantitative reverse transcriptase PCR. Total RNA was purified from cell lysates with RNeasy mini kit (QIAGEN GmbH) according to manufacturer's instructions. cDNA synthesis was carried out with reagents and devices from Applied Biosystems. Quantitative RT-PCR based on TaqMan method was applied to determine xCT mRNA level in the cell samples. xCT mRNA level was normalized to hydroxymethylbilane synthase (HMBS) mRNA as internal control.

Gene expression assay for human *xCT*: Hs00204928_m1 (Applied Biosystems)
Gene expression assay for human HMBS: Hs00609297_m1 (Applied Biosystems)

In vivo animal studies

All animal experiments were carried out in compliance with the current version of the German law concerning animal protection and welfare. PET imaging and biodistribution experiments were carried out with tumor-bearing mice or rats. NMRI nude mice (Taconic) or nude rats (RH-Foxn1 nu/nu; Harlan-Winkelmann) were used for subcutaneous inoculation of human xenografts. Female Fischer rats were obtained from Charles River and used for the combined tumor and turpentine oil inflammation model. For this model the syngenic rat GS9L glioblastoma cell line was used.

Tumor cells (2–5 $\times$ 10^6 cells per mouse) were injected subcutaneously and allowed to grow for 1 to 4 weeks. The tumor size at the time of the animal study was in the range of 60 to 200 mg. For biodistribution studies, 185 kBq of BAY 94-9392 in 100 μL PBS buffer was injected intravenously in conscious animals via the tail vein. Food and water was available *ad libitum*. Animals were sacrificed at various times (0.25–2 hours; $n = 3$ for each time point). Organs and tissues of interest were collected and weighed. The amount of radioactivity was determined with the gamma counter to calculate uptake as the percentage of injected dose per gram of tissue (%ID/g). The mean %ID/g value and SD were calculated from 3 animals for each time point.

PET imaging studies with tumor-bearing rats were carried out using the Inveon small animal PET/computed

tomography (CT) scanner (Siemens). Nude rats were inoculated with 5×10^6 NCI-H460 tumor cells in 100 μL matrigel in the right flank. Ten to 16 MBq of BAY 94-9392 were injected intravenously in conscious animals via the tail vein. Eighty-five minutes postinjection (p.i.) the animals were anesthetized with isoflurane (Abbot) and the PET data were acquired from 90 to 110 minutes p.i. Rat GS9L glioblastoma tumor cells (2×10^6 cells in a volume of 100 μL of medium + matrigel) were inoculated subcutaneously into the right hind leg. Five days post-GS9L tumor cell inoculation all animals received an injection of 100 μL turpentine oil in the left calf muscle. PET imaging using either FDG or BAY 94-9392 was carried out 72 hours postinduction of the inflammation. No fasting was applied for both groups prior to tracer injection. Animals receiving FDG were kept anaesthetized with isoflurane and warmed for the whole distribution period to avoid confounding tracer uptake in muscle tissue because of locomotor activity. PET data from both groups were acquired from 60 to 70 minutes postinjection. After finishing PET data acquisition the animals were sacrificed, the inflamed muscle and contralateral muscle tissue were removed, weighed, and radioactivity was determined with a gamma counter to calculate the uptake as %ID/g. The mean %ID/g value and the SD were calculated from 3 animals, each. For subsequent histopathologic analysis muscle samples were formalin fixed and paraffin embedded. Hematoxylin and eosin staining and immunohistochemistry using the CD68 antibody (Serotec MCA341R) for macrophage staining were carried out using established standard protocols.

Results

In vitro studies: identification of BAY 94-9392

Substituted L-glutamate derivatives were investigated in cell competition assays to gain insights in structure–activity relationships of the involved transporter(s). These nonradioactive compounds were tested in large molar excess for their ability to compete with the uptake of a previously described radioabeled L-glutamate derivative (27). Competition data are summarized in Table 1. Coincubation of the radiotracer with L-glutamate and L-cystine strongly reduced the tracer uptake to 9.7% and 9.9%, respectively, pointing to the involvement of system x_C^-. No competition (95.6% uptake of control) was determined by coincubation with 2-ethyl glutamate. Substitution in 3-position reduced radiotracer uptake to 33.7% or 51.8% when incubated with 3-hydroxyl-glutamate or (±)-threo-3-methyl glutamate, respectively. 4-substituted glutamate derivatives showed high competition (5.4%–33.5% uptake). 4*S*-configurated methyl and hydroxyl derivatives showed higher competition (7.7% and 13.2%) than the 4*R*-configurated derivatives (29.5% and 33.5%). Strong competition was observed with the 4*S*-fluoropropyl derivative [^{19}F]-BAY 94-9392 (5.4%).

[^{19}F]-BAY 94-9392 was further studied in a dose-dependent manner for competition against the natural radiolabeled substrates of system x_C^-, [^{3}H]L-glutamate, and [^{14}C]L-cystine. IC_{50} values of 29.1 and 33.6 μmol/L were determined for [^{19}F]-BAY 94-9392 (Fig. 2A and B). These values are lower than the values determined for L-glutamate and L-cystine (111.7 and 116.4 μmol/L, respectively).

To get access to the ^{18}F-labeled fluoropropyl derivative, an automated radiosynthesis was established using a nosylate precursor. (4*S*)-(3-[^{18}F]fluoropropyl)-L-glutamate (BAY 94-9392) was obtained in a radiochemical yield of more than 40% decay corrected and purity of more than 92% ($n = 40$). For more details see Supplementary data.

In vitro studies: characterization of BAY 94-9392 uptake and retention

The uptake of BAY 94-9392 was investigated in different tumor cell lines. Time dependency of uptake is shown in Figure 2C for the human lung tumor cell line NCI-H460. An equilibrium was reached after 60 minutes of incubation at which time approximately 16% of the applied dose was internalized. Representative tumor cell lines were investigated and showed an uptake with values ranging from 1% to 18% uptake per 100,000 cells in 30 minutes (Fig. 2D). Highest uptake was observed in the human non–small-cell lung carcinoma cell line NCI-H322 with 18.3% per 100,000 cells. Prostate cancer 22RV1 cells and liver cancer HepG2 showed lower uptake (1.7% and 1.4% uptake per 100,000 cells, respectively).

To further characterize the responsible transporter for cellular uptake of BAY 94-9392, tracer uptake was investigated in the presence of structurally similar compounds. Strong inhibition of BAY 94-9392 uptake (~80%) was observed by coincubation with an excess of either L-glutamate, L-cystine, or the system x_C^--specific inhibitor p-carboxy-phenylglycine (CPG), but not by L- or D-aspartate. The competition profile for NCI-H460 cells is shown as an example in Figure 3A and indicates specific uptake through system x_C^-. To further show that uptake of BAY 94-9392 proceeds via this transport system, knockdown cells were generated using the human A549 lung tumor cell line. mRNA levels of the xCT subunit of system x_C^- were reduced to 14% to 18% in the A549 cell subclones carrying 2 independent shRNA sequences, sh1487 and sh7701, respectively. Knockdown cells were viable and showed slightly reduced proliferation (44%–56%) compared with the parental cell line (see Supplementary information). BAY 94-9392 cell uptake was reduced to 29.7% and 38.0% compared with mock-treated cells. Thus, xCT knockdown reduces the capacity for initial uptake of BAY 94-9392 via system x_C^- (Fig. 3B).

The intensity of a tumor PET signal *in vivo* depends on rapid and high uptake as well as strong retention. To study intracellular retention and metabolism, BAY 94-9392–loaded cells were investigated under efflux conditions. In PBS buffer containing no transporter substrates approximately 80% of the initial tracer uptake is retained in tumor cells. Incubation with PBS buffer containing excess of L-glutamate, ^{19}F-BAY 94-9392, or complete minimum essential medium (MEM) medium with L-cystine caused release of intracellular radioactivity within 30 minutes. High

Table 1. Structure activity relationship of glutamate derivatives

Compound (1 mmol/L)	Structure	Uptake of BAY 85-8050
None		100 ± 3.4
L-glutamate	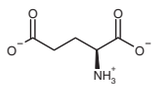	9.7 ± 1.0
L-cystine[a]	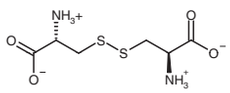	9.9 ± 1.5
2-ethyl-glutamate	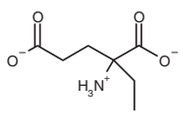	95.6 ± 8.6
3-hydroxy-glutamate	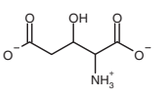	33.7 ± 2.3
(+/-)-threo 3-methyl-glutamate	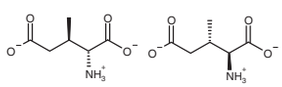	51.8 ± 4.3
(4*S*)-hydroxy-L-glutamate	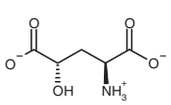	13.2 ± 1.8
(4*R*)-hydroxy-L-glutamate	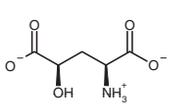	29.6 ± 4.2
(4*S*)-methyl-L-glutamate	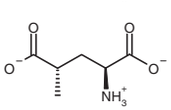	7.7 ± 1.9
(4*R*)-methyl-L-glutamate	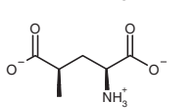	33.5 ± 5.5
4,4-dimethyl-L-glutamate	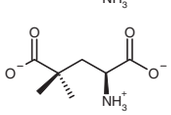	33.1 ± 0.6
4-fluoro-D/L-glutamate	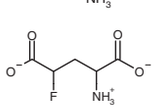	16.3 ± 2.5
^{19}F-BAY94-9392 (4*S*)-fluoropropyl-L-glutamate	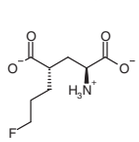	5.4 ± 2.2

NOTE. Uptake of BAY 85-8050 (4-[^{18}F]fluoroglutamate) (ref. 27) in A549 cells in the presence and absence of glutamate derivatives (1 mmol/L) or L-cystine. Values are reported as % of control (mean, $n = 3$, ± SD).

[a]L-cystine was studied at 0.8 mmol/L because of its limited solubility.

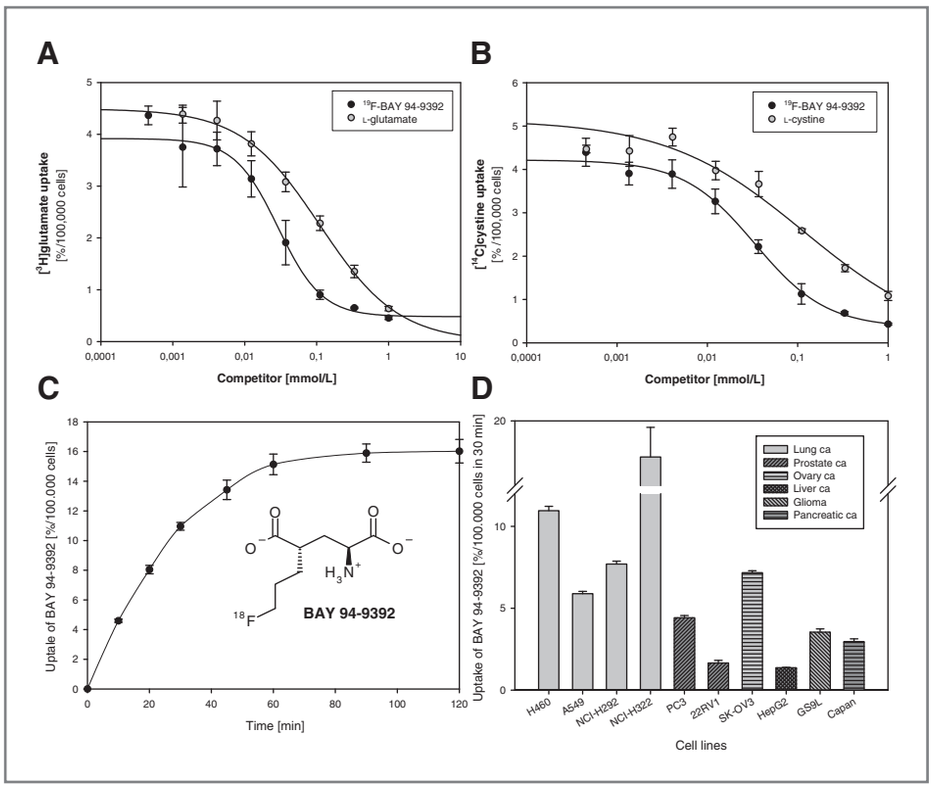

Figure 2. *In vitro* characterization of (4*S*)-(3-fluoropropyl)-L-glutamate and its ^{18}F-radiolabeled derivative BAY 94-9392. A and B, dose-dependent competition cell uptake assays were carried out in human NCI-H460 lung cancer cells using the ^{19}F-derivative of BAY 94-9392 and the radiolabeled natural xCT substrates [^{3}H]L-glutamate and [^{14}C]L-cystine. C, time-dependent uptake of BAY 94-9392 in NCI-H460 lung tumor cells was monitored for 120 minutes. D, overview of representative tumor cell lines used for BAY 94-9392 cell uptake studies. Uptake of BAY 94-9392 was determined after 30-minute incubation.

retention was observed after incubation of the cells with MEM plus mercaptoethanol or with PBS containing the inhibitors of system x_C^-, CPG, or sulfasalazine (Fig. 3C). Thin-layer chromatography (TLC) of the cell lysates and released radioactivity in the supernatant revealed exclusive presence of the parent compound (data not shown).

In vivo studies: pharmacokinetics and tumor targeting

Tumor uptake and biodistribution of BAY 94-9392 were assessed in tumor-bearing animals. After tracer injection in conscious animals, the animals had access to water and food *ad libitum*. During the distribution period, anesthesia was not necessary for BAY 94-9392, whereas for FDG anesthesia is recommended to avoid its high uptake in muscle and brown fat (28). The results are expressed as %ID and are normalized for tissue weight in gram. Quantitative and kinetic analysis of the BAY 94-9392 uptake in NCI-H460 tumors in mice reveal a rapid and high initial tumor uptake which remains constant at a high level (4.1% ± 1.4% ID/g at 0.25 hour p.i. and 3.2% ± 0.4% ID/g at 1 hour p.i.). Rapid blood clearance via the kidneys was observed resulting in a high tumor-to-blood ratio of 14 and a tumor-to-muscle ratio of 27 at 1 hour p.i. The pancreas showed an initial uptake of 19.4% ± 4.2% ID/g at 0.25 hour p.i. decreasing to 5.8% ± 0.9% ID/g at 1 hour p.i. Other organs of interest such as the brain, liver, and muscle showed negligible or low uptake (<1% ID/g; Fig. 4A). The bone signal remains less than 1% ID/g over time indicating no defluorination of BAY 94-9392. The analysis of potential metabolites of BAY 94-9392 was carried out in blood samples at different time points. Only the parent compound was detectable by TLC analysis (see also Supplementary information). The tumor uptake of BAY 94-9392 was investigated in a panel of other subcutaneous human tumor models in mice. Most of the tumors showed an uptake in the range of 2% to 4% ID/g at 60 minutes p.i. (Fig. 4B). These tumor uptake values together with low background signals and rapid clearance provide high contrast for tumor imaging. Comparable or slightly higher tumor uptake values were observed for FDG in animal models. However, FDG is very sensitive for study conditions and some prerequisites need to be considered. For example, if mice were kept under anesthesia and warmed after tracer injection, NCI-H460 tumors in mice showed a FDG uptake of 4.0% ± 0.4% ID/g yielding a tumor to blood ratio of 8. If no anesthesia was applied, the FDG uptake in NCI-H460 tumors dropped to 1.8% ± 0.2% ID/g, whereas other organs and tissues like muscle and brown fat showed increased uptake (unpublished own data). In contrast, for BAY 94-9392 no influence of animal handling conditions such as anesthesia and locomotor activity was observed on tumor uptake.

In vivo studies: PET imaging

PET/CT imaging was carried out with BAY 94-9392 in human NCI-H460 tumor-bearing rats. Almost exclusive tracer accumulation was observed in the tumor, kidney, and the pancreas relative to all other normal tissues

(Fig. 4C). FDG was investigated under analogous conditions and showed higher background signals arising from its uptake in muscle, brain, intestine, brown fat, and other tissues (see also Supplementary data).

To test whether inflammatory processes would also accumulate BAY 94-9392, the tracer uptake was investigated in a combined tumor and inflammation model. Immunocompetent rats were used bearing a rat GS9L glioblastoma subcutaneously in one leg. An inflammatory process was initiated in the contralateral calf muscle using turpentine oil. Both, BAY 94-9392 and FDG showed uptake in the GS9L tumors. However, BAY 94-9392 showed negligible uptake in inflammatory lesions (0.18% ± 0.02% ID/g, $n = 3$, Fig. 5A) compared with the uptake of FDG (1.95% ± 0.18% ID/g, $n = 3$, Fig. 5B). Histopathologic analysis confirmed similar extent of inflammation with massive invasion of neutrophils and macrophages in all animals (Fig. 5C).

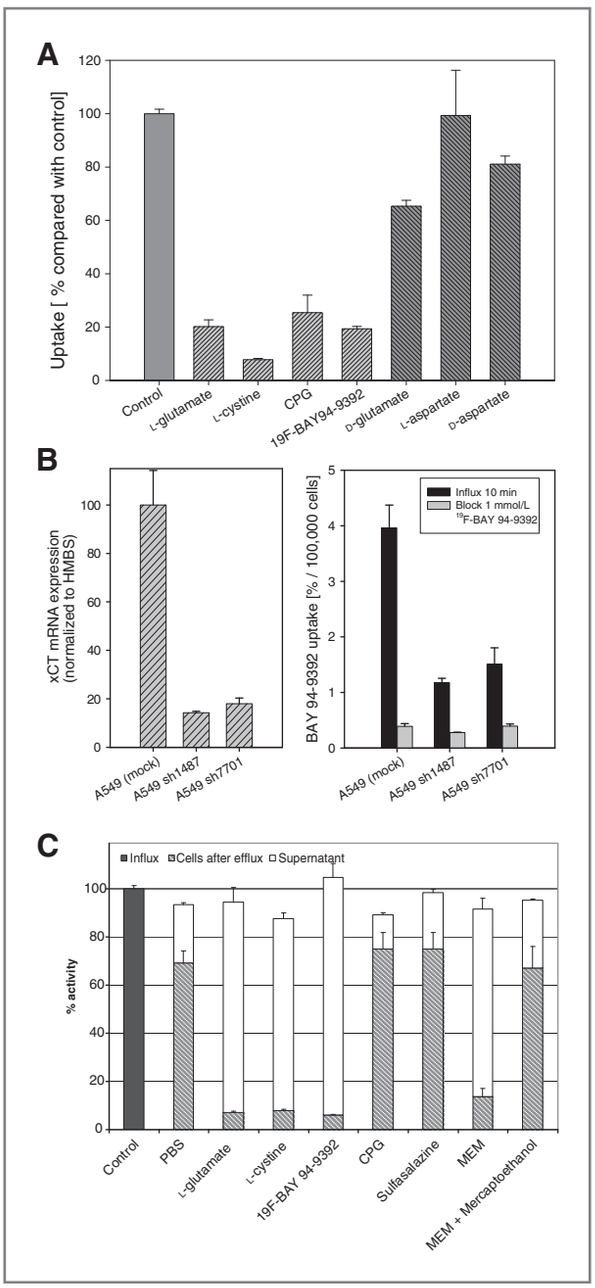

Discussion

Adaptations of tumor metabolism offer opportunities to provide more specific PET tracers for tumor imaging and to overcome limitations of FDG. In this context, the system x_C^- plays an important role in tumors by providing an efficient access to L-cystine conferring a selective advantage for growth and survival. Substituted glutamate derivatives were investigated in cell competition assays for their interaction with system x_C^-. It was observed that 4-substituted glutamate derivatives showed high competition with radiolabeled glutamate compared to substituted compounds in 2- and 3-position. A fluoropropyl-substituted derivative (^{19}F-BAY 94-9392) showed strong competition with low IC_{50} values. This derivative was chosen based on its high affinity to system x_C^- and its accessibility for incorporation of a radioactive fluorine-18 atom. An efficient radiosynthesis was established to produce the ^{18}F-radiolabeled derivative BAY 94-9392 that can be used for tumor PET imaging as well as to trace its transport and retention in tumor cells. Time-dependent uptake was observed that reached a plateau after 60 minutes, indicating a transporter-mediated uptake. In general, a high uptake of BAY 94-9392 was observed in several tumor cell lines from different entities with variations in the absolute amounts. Specific transport of BAY 94-9392 via system x_C^- was revealed by strong competition of tracer uptake with L-glutamate and L-cystine as well as with the xCT subunit-specific inhibitor CPG. Only minor competition was observed with either D- and L-aspartate which are both substrates along with L-glutamate for the EAAT family members 1–5. In addition, the specificity of BAY 94-9392 transport and dependency

Figure 3. Identification and characterization of the transporter responsible for cellular uptake of BAY 94-9392. A, coincubation of NCI-H460 cells was carried out with BAY 94-9392 as ^{18}F-radiotracer and several structurally similar compounds in excess (1 mmol/L) for 10 minutes in PBS buffer. Strong inhibition of tracer uptake was observed with L-glutamate, L-cystine, and the xCT subunit inhibitor CPG and the nonradioactive derivative ^{19}F-BAY 94-9392 indicating uptake through system x_C^-. Negligible competition was observed with L- and D-aspartate confirming no or minor involvement of glutamate transporters from the excitatory amino acid transporter family. B, xCT shRNA knockdown cells were generated using the human A549 lung cancer cell line. xCT knockdown clones sh1487 and sh7701 showed a reduced uptake of BAY 94-9392 compared with mock-treated A549 cells. C, intracellular retention of BAY 94-9392 was investigated in a trans-stimulation assay. NCI-H460 cells were loaded with BAY 94-9392 for 30 minutes. Cells were washed and reincubated with different compounds at 1 mmol/L concentration. Intracellular and the released radioactivity into the supernatant were measured. Strong release of radioactivity was observed only in the presence of excess amounts of putative substrates for system x_C^-. Inhibitors of system x_C^- such as CPG or sulfasalazine are not able to release activity from BAY 94-9392–loaded cells.

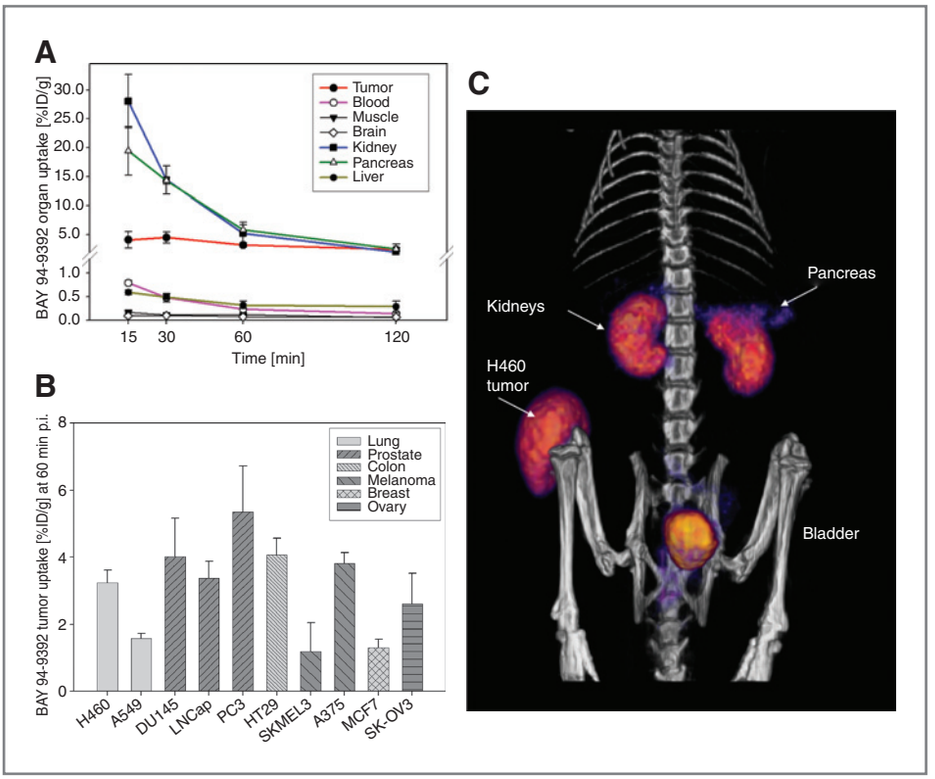

Figure 4. Pharmacokinetics, biodistribution, and tumor targeting of BAY 94-9392. A, biodistribution and pharmacokinetics of BAY 94-9392 were analyzed in NCI-H460 tumor-bearing mice. The time course of BAY 94-9392 signal is shown for tumor as well as for selected organs and tissues. A sustained tumor signal at a high level and rapid clearance from most healthy organs and tissues was observed. Only the kidneys and the pancreas showed still increased levels of BAY 94-9392 at later time points. B, tumor uptake of BAY 94-9392 was investigated in a panel of other subcutaneous human tumor models in mice. Tracer uptake at 60 minutes p.i. is displayed. Most tumors showed an uptake level between 2% and 4% ID/g. C, human NCI-H460 lung tumor-bearing rats were used for tumor visualization by PET. Surface rendered whole body PET data (in yellow-red) were acquired from 90 to 110 minutes p.i. and fused with the CT image (in grey). A strong tumor signal and low background from healthy tissues were confirmed by PET. In addition to the tumor signal, only the kidneys and the bladder as excretion organs as well as the pancreas are visible. A rotating image is available in the supplementary information.

of system x_C^- expression level was investigated using 2 different stable knockdown cell clones of the xCT subunit from the A549 lung cancer cell line. Reduced mRNA levels of xCT led to a reduced capacity for uptake of BAY 94-9392.

A strong intracellular retention of BAY 94-9392 was observed in PBS buffer in the absence of putative exchange substrates for system x_C^- indicating no further involvement of other efflux mechanisms. However, in the presence of excess transporter substrates such as L-glutamate, L-cystine, or ^{19}F-BAY 94-9392 in the efflux buffer, a complete exchange of the intracellular glutamate can be observed as traced by an almost complete release of intracellular radioactivity. Obviously, no intracellular metabolism of BAY 94-9392 occurs and therefore it can exit the cells only via system x_C^-. TLC analyses confirmed the presence of the parent compound in the cell lysates and supernatants as the sole component. Taken together, these *in vitro* experiments clearly indicate that even without an intracellular enzymatic conversion a high retention in tumor cells can be achieved. This is markedly different from FDG's cellular retention in which its phosphorylation is required to prevent subsequent efflux (29).

To test the hypothesis that system x_C^- activity is an important pathway in tumors compared with other tissues, biodistribution as well as PET imaging studies of tumor-bearing animals were carried out. The rapid and high tumor uptake of BAY 94-9392 together with a rapid clearance from blood and other healthy tissues led to excellent tumor visualization for at least 2 hours p.i. Broad applicability of this PET tracer for tumor imaging was shown by analysis of other human tumor models in mice. Even tumors with rather low total uptake values, such as A549 (1.6% ID/g at 60 minutes p.i.) can be well visualized by PET in mice (data not shown) because of the favorable low background.

For a better understanding of the sustained BAY 94-9392 tumor signal, the source and metabolic fate of intracellular L-glutamate needs further consideration. The blood concentration of L-glutamate is approximately 50 μmol/L and similar to L-cystine concentration (30, 31). However, high intracellular concentrations of L-glutamate up to 20 mmol/L have been reported in tumors (19). The majority of intracellular L-glutamate is derived from L-glutamine which is the most abundant amino acid in the blood. It is

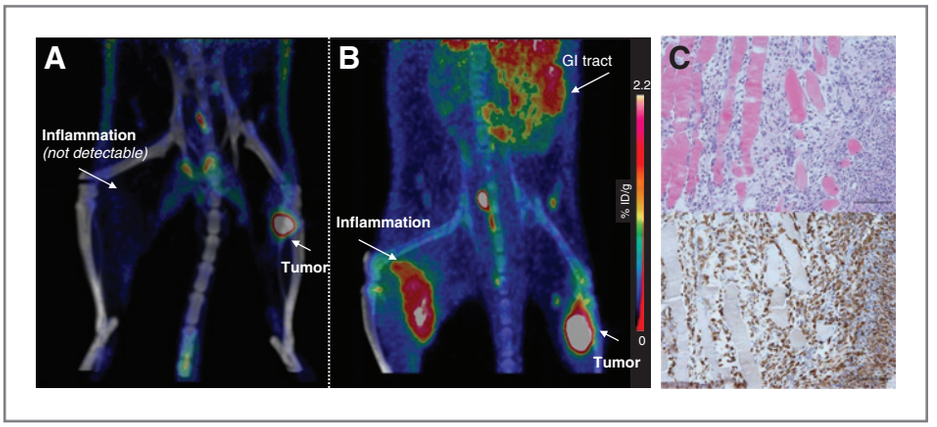

Figure 5. Investigation of BAY 94-9392 and FDG in a combined rat GS9L glioblastoma and inflammation model by PET/CT imaging in rats. PET imaging was carried out 72 hours after turpentine oil injection with either BAY 94-9392 or with FDG. Whole-body PET data (colored) were acquired from 60 to 70 minutes p.i. and fused with the CT image. A, BAY 94-9392 showed strong accumulation in GS9L tumors but no detectable uptake in the inflammatory lesions. B, FDG accumulates in both the tumor and inflammation. In addition, a higher uptake was observed for FDG in the gastrointestinal (GI) tract compared with BAY 94-9392. C, histopathologic analysis of the inflamed muscle samples showed presence of central necrosis with destructed muscle tissue and massive invasion of neutrophils (top). CD68 immunohistochemistry was carried out to stain macrophages (bottom).

well known that proliferating cells have a high demand for this amino acid. Efficient supply of L-glutamine in tumors is mediated by a set of different transporters, in particular ASCT2 (SLC1A5; ref. 32). The high uptake of L-glutamine and its subsequent deamination by glutaminase form the basis for a high intracellular concentration of glutamate. Recently, data were published about the radiosynthesis of ^{18}F-glutamine derivatives to study this process (33). The carbon backbone of glutamine is similar to glutamate, but different transporters and a different metabolic pathway are being addressed. As several anabolic pathways, in particular the lipogenesis pathway, are responsible for depletion of TCA cycle intermediates, there is a high demand for anaplerosis which can be met in part by L-glutamate. The high intracellular concentration of L-glutamate in tumors assures constant availability of an exchange substrate and promotes system x_C^- operation at a high activity. The dependency of x_C^- activity on the intracellular glutamate concentration was studied with human fibroblasts using [^{3}H]L-cystine as radiotracer. Fibroblasts were incubated in glutamine-/glutamate-free medium for up to 24 hours. Glutamate levels dropped within 3 hours which was paralleled by a reduced rate of [^{3}H]L-cystine uptake (16). However, our *in vivo* experiments showed high uptake of BAY 94-9392 in multiple tumor models and a rather constant tumor signal over time. This indicates the presence of a high x_C^- activity along with a robust and high intracellular concentration of glutamate as a common feature of tumors. Thus, BAY 94-9392 gets diluted in the large intracellular glutamate pool conferring tracer retention in the cells without need for enzymatic processing. Only if an excess of extracellular exchange substrates is provided to the tracer-loaded cells, a complete exchange of intracellular glutamate can be achieved concomitant with a release of BAY 94-9392.

A critical issue is the understanding of the relative role of transporter expression and changes of flux in tumor cells. Comprehensive studies to correlate the uptake and retention of BAY 94-9392 with mRNA levels of system x_C^-, the transporter (subunit) density and activity at protein level as well as glutamate concentrations are currently ongoing. Previously published data indicate the importance of system x_C^- for mediating chemoresistance of melphalan, cisplatin, irinotecan, and celastrol (34–38). In addition, an interaction of the xCT subunit of system x_C^- with a variant of the cancer stem cell marker CD44 was published recently. CD44v contributes to the regulation of the redox status in tumors by stabilizing the xCT subunit and promotes tumor growth (39). Ablation of CD44v induced loss of xCT from the cell surface and suppressed tumor growth in a transgenic mouse model of gastric cancer. In future studies, BAY 94-9392 might not only be used for more specific tumor detection, but can also be employed as novel tool for the noninvasive assessment of tumors redox balance and thiol-mediated detoxification potential.

In addition to its role in the tumor metabolism, elevated expression of system x_C^- has been reported in activated macrophages *in vitro* but not in tumor-associated macrophages (40, 41). The turpentine oil inflammation model has been used extensively to model sterile inflammation and accumulation of macrophages (42). However, no accumulation of BAY 94-9392 was observed in histopathologically proven inflammatory lesions containing massive invasion of neutrophiles and macrophages. Thus, the tracer uptake in neutrophils and macrophages via system x_C^- does not seem to be a dominant mechanism in this particular *in vivo* inflammation model.

In conclusion, system x_C^- is an important transporter in tumor cells. Its critical role in malignant transformation can be exploited to develop imaging and therapeutic agents. The ^{18}F-radiolabeled glutamate derivative BAY 94-9392 is a metabolically stable PET tracer in rodents.

It is specifically taken up via system x_C^- and strongly retained in tumors. PET imaging of system x_C^- activity using BAY 94-9392 has a potential for not only improving early detection and staging of several tumors with higher sensitivity and specificity than FDG, but also guiding therapeutic interventions by imaging metabolic adaptations to oxidative stress *in vivo*. More studies are needed to further elucidate and correlate the uptake pattern of BAY 94-9392 with underlying chemoresistance mechanisms. Clinical studies using BAY 94-9392 are in progress to characterize this compound in cancer patients. Ongoing implementation of such new PET tracers raises hopes of being able to better detect and characterize unique adaptive and metabolic pathways within malignant tissues.

Disclosure of Potential Conflicts of Interest

No potential conflicts of interest were disclosed.

Acknowledgments

The skillful technical assistance of research staff at Bayer HealthCare, Berlin is gratefully acknowledged. We thank Manfred K. Grieshaber, Institute of Biochemistry, University of Düsseldorf, for stimulating scientific discussions about glutamate metabolism and adaptive biochemical mechanisms. We are grateful to Anna-Lena Frisk for carrying out immunohistochemistry analyses.

The costs of publication of this article were defrayed in part by the payment of page charges. This article must therefore be hereby marked *advertisement* in accordance with 18 U.S.C. Section 1734 solely to indicate this fact.

Received March 14, 2011; revised June 15, 2011; accepted June 30, 2011; published OnlineFirst July 12, 2011.

References

1. Warburg O, Posener K, Negelein E. Über den Stoffwechsel der Carcinomzelle. Biochem Z 1924;152:309–44.
2. DeBerardinis RJ, Lum JJ, Hatzivassiliou G, Thompson CB. The biology of cancer: metabolic reprogramming fuels cell growth and proliferation. Cell Metab 2008;7:11–20.
3. Vander Heiden MG, Locasale JW, Swanson KD, Sharfi H, Heffron GJ, Amador-Noguez D, et al. Evidence for an alternative glycolytic pathway in rapidly proliferating cells. Science 2010;329:1492–99.
4. Cairns RA, Harris IS, Mak TW. Regulation of cancer cell metabolism. Nat Rev Cancer 2011;11:85–95.
5. Mankoff DA, Eary JF, Link JM, Muzi M, Rajendran JG, Spence AM, et al. Tumor-specific positron emission tomography imaging in patients: [18F] fluorodeoxyglucose and beyond. Clin Cancer Res 2007;13:3460–69.
6. Weber WA, Grosu AL, Czernin J. Technology insight: advances in molecular imaging and an appraisal of PET/CT scanning. Nat Clin Pract Oncol 2008;5:160–70.
7. Shreve PD, Anzai Y, Wahl RL. Pitfalls in oncologic diagnosis with FDG PET imaging: physiologic and benign variants. RadioGraphics 1999;19:61–77.
8. Okuno S, Sato H, Kuriyama-Matsumura K, Tamba M, Wang H, Sohda S, et al. Role of cystine transport in intracellular glutathione level and cisplatin resistance in human ovarian cancer cell lines. Br J Cancer 2003;88:951–6.
9. Meister A. Glutathione metabolism. Methods Enzymol 1995;251:3–7.
10. Ogunrinu TA, Sontheimer H. Hypoxia increases the dependence of glioma cells on glutathione. J Biol Chem 2010;285:37716–24.
11. Banjac A, Perisic T, Sato H, Seiler A, Bannai S, Weiss N, et al. The cystine/cysteine cycle: a redox cycle regulating susceptibility versus resistance to cell death. Oncogene 2008;27:1618–28.
12. Olm E, Fernandes AP, Hebert C, Rundlöf AK, Larsen EH, Danielsson O, et al. Extracellular thiol-assisted selenium uptake dependent on the x(c)- cystine transporter explains the cancer-specific cytotoxicity of selenite. Proc Natl Acad Sci U S A 2009;106:11400–5.
13. Bannai S, Kitamura E. Transport interaction of L-cystine and L-glutamate in human diploid fibroblasts in culture. J Biol Chem 1980;255:2372–76.
14. Bassi MT, Gasol E, Manzoni M, Pineda M, Riboni M, Martín R, et al. Identification and characterisation of human xCT that co-expresses, with 4F2 heavy chain, the amino acid transport activity system xc-. Pflugers Arch 2001;442:286–96.
15. Verrey F, Closs EI, Wagner CA, Palacin M, Endou H, Kanai Y. CATs and HATs: the SLC7 family of amino acid transporters. Pflugers Arch 2004;447:532–42.
16. Bannai S. Exchange of cystine and glutamate across plasma membrane of human fibroblasts. J Biol Chem 1986;261:2256–63.
17. Patel SA, Warren BA, Rhoderick JF, Bridges RJ. Differentiation of substrate and non-substrate inhibitors of transport system xc(-): an obligate exchanger of L-glutamate and L-cystine. Neuropharmacology 2004;46:273–84.
18. Lo M, Wang YZ, Gout PW. The x(c)- cystine/glutamate antiporter: a potential target for therapy of cancer and other diseases. J Cell Physiol 2008;215:593–602.
19. DeBerardinis RJ, Mancuso A, Daikhin E, Nissim I, Yudkoff M, Wehrli S, et al. Beyond aerobic glycolysis: transformed cells can engage in glutamine metabolism that exceeds the requirement for protein and nucleotide synthesis. Proc Natl Acad Sci U S A 2007;104:19345–50.
20. Aledo JC. Glutamine breakdown in rapidly dividing cells: waste or investment?Bioessays 2004;26:778–85.
21. Ametamey SM, Honer M, Schubiger PA. Molecular imaging with PET. Chem Rev 2008;108:1501–16.
22. Gout PW, Buckley AR, Simms CR, Bruchovsky N. Sulfasalazine, a potent suppressor of lymphoma growth by inhibition of the x(c)- cystine transporter: a new action for an old drug. Leukemia 2001;10:1633–40.
23. Krause BJ, Smolarz K, Graner FP, Wagner F, Wester HJ, Kleinhempel T, et al. [18F]BAY 85-8050 (TIM-1): a novel tumor specific probe for PET/CT imaging - First clinical results. J Nucl Med 2010;51 Suppl 2:118.
24. Belvisi L, Colombo L, Colombo M, Di Giacomo M, Manzoni L, Vodopivec B, et al. Practical stereoselective synthesis of conformationally constrained unnatural proline-based amino acids and peptidomimetics. Tetrahedron 2001;57:6463–73.
25. Han G, Tamaki M, Hruby VJ. Fast, efficient and selective deprotection of the tert-butoxycarbonyl (Boc) group using HCl/dioxane (4 M). J Peptide Res 2001;58:338–41.
26. Berndt M, Schmitt-Willich H, Friebe M, Graham K, Brumby T, Hultsch C, et al. Method for production of F-18 labeled glutamic acid derivatives (Bayer Schering Pharma Aktiengesellschaft), WO 2011/060887.
27. Krasikova RN, Kuznetsova OF, Fedorova OS, Belokon YN, Maleev VI, Mu L, et al. 4-[(18)F]Fluoroglutamic acid (BAY 85-8050), a new amino acid radiotracer for PET imaging of tumors: synthesis and in vitro characterization. J Med Chem 2011;54:406–10.
28. Fueger BJ, Czernin J, Hildebrandt I, Tran C, Halpern BS, Stout D, et al. Impact of animal handling on the results of 18F-FDG PET studies in mice. J Nucl Med 2006;47:999–1006.
29. Landau BR, Spring-Robinson CL, Muzic RF Jr, Rachdaoui N, Rubin D, Berridge MS, et al. 6-Fluoro-6-deoxy-D-glucose as a tracer of glucose transport. Am J Physiol Endocrinol Metab 2007;293:E237–45.
30. Hack V, Schmid D, Breitkreutz R, Stahl-Henning C, Drings P, Kinscherf R, et al. Cystine levels, cystine flux, and protein catabolism in cancer cachexia, HIV/SIV infection, and senescence. FASEB J 1997;11:84–92.
31. Le Boucher J, Charret C, Coudray-Lucas C, Giboudeau J, Cynober L. Amino acid determination in biological fluids by automated

ion-exchange chromatography: performance of Hitachi L-8500A. Clin Chem 1997;43:1421–28.
32. DeBerardinis RJ, Cheng T. Q's next: the diverse functions of glutamine in metabolism, cell biology and cancer. Oncogene 2010; 29:313–24.
33. Qu W, Zha Z, Ploessl K, Lieberman BP, Zhu L, Wise DR, et al. Synthesis of optically pure 4-fluoro-glutamines as potential metabolic imaging agents for tumors. J Am Chem Soc 2011;133:1122–33.
34. Awasthi S, Sharma R, Singhal SS, Herzog NK, Chaubey M, Awasthi YC. Modulation of cisplatin cytotoxicity by sulphasalazine. Br J Cancer 1994;70:190–4.
35. Huang Y, Dai Z, Barbacioru C, Sadée W. Cystine-glutamate transporter SLC7A11 in cancer chemosensitivity and chemoresistance. Cancer Res 2005;65:7446–54.
36. Dai Z, Huang Y, Sadee W, Blower P. Chemoinformatics analysis identifies cytotoxic compounds susceptible to chemoresistance mediated by glutathione and cystine/glutamate transport system xc-. J Med Chem 2007;50:1896–1906.
37. Chintala S, Tóth K, Yin MB, Bhattacharya A, Smith SB, Ola MS, et al. Downregulation of cystine transporter x(c) by irinotecan in human head and neck cancer FaDu xenografts. Chemotherapy 2010;56: 223–33.
38. Pham AN, Blower PE, Alvarado O, Ravula R, Gout PW, Huang Y. Pharmacogenomic approach reveals a role for the x(c)- cystine/glutamate antiporter in growth and celastrol resistance of glioma cell lines. J Pharmacol Exp Ther 2010;332:949–58.
39. Ishimoto T, Nagano O, Yae T, Tamada M, Motohara T, Oshima H, et al. CD44 variant regulates redox status in cancer cells by stabilizing the xCT subunit of system xc(-) and thereby promotes tumor growth. Cancer Cell 2011;19:387–400.
40. Nabeyama A, Kurita A, Asano K, Miyake Y, Yasuda T, Miura I, et al. xCT deficiency accelerates chemically induced tumorigenesis. Proc Natl Acad Sci USA 2010;107:6436–41.
41. Sato H, Kuriyama-Matsumura K, Hashimoto T, Sasaki H, Wang H, Ishii T, et al. Effect of oxygen on induction of the cystine transporter by bacterial lipopolysaccharide in mouse peritoneal macrophages. J Biol Chem 2001;276:10407–12.
42. Yamada S, Kubota K, Kubota R, Ido T, Tamahashi N. High accumulation of fluorine-18-fluorodeoxyglucose in turpentine-induced inflammatory tissue. J Nucl Med 1995;36:1301–6.
43. Menendez JA, Lupu R. Fatty acid synthase and the lipogenic phenotype in cancer pathogenesis. Nat Rev Cancer 2007;7:763–77.
44. Mazurek S, Boschek CB, Hugo F, Eigenbrodt E. Pyruvate kinase type M2 and its role in tumor growth and spreading. Semin Cancer Biol 2005;15:300–8.
45. Christofk HR, Vander Heiden MG, Harris MH, Ramanathan A, Gerszten RE, Wei R, et al. The M2 splice isoform of pyruvate kinase is important for cancer metabolism and tumour growth. Nature 2008;452:230–3.
46. Vander Heiden MG, Locasale JW, Swanson KD, Sharfi H, Heffron GJ, Amador-Noguez D, et al. Evidence for an alternative glycolytic pathway in rapidly proliferating cells. Science 2010;329: 1492–99.
47. Cheng T, Sudderth J, Yang C, Mullen AR, Jin ES, Matés JM, et al. Pyruvate carboxylase is required for glutamine-independent growth of tumor cells. Proc Natl Acad Sci U S A 2011;108:8674–9.